Separation of an incoming and reflecting impulse for determining angle-dependent acoustic properties in situ

Jochen Metzger, Stefan Tschallener and Manfred Kaltenbacher
TU Wien, 1060 Wien, Austria, Email: jochen.metzger@tuwien.ac.at

Introduction

For precisely obtaining an acoustic field close to reality, the acoustic wave equation with realistic boundary conditions has to be solved. Therefore, the knowledge of these acoustic boundary conditions is crucial. By applying the standardized measurement methods, only the absorption at random sound incidence [1] and perpendicular sound incidence [2] can be obtained. Furthermore, those methods need for a trimmed sample with special size and dimensions. However, no real sound excitation will be a perfect plane wave or a diffuse sound field and the cutting process (if it is possible at all) may change the acoustic behavior. To determine the acoustic properties at the location where the material is installed, in situ measurement techniques are beneficial. Several in situ approaches can be found in literature [3]. For the measurements presented in this paper, a subtraction method as described in [8] is used. Besides the method discussed in this paper, a variety of other approaches exist, e.g. a method which uses a spatial Fourier transformation for the determination of the sound pressure reflection coefficient [4] [5], a two microphone method, which determines the normal acoustic impedance at oblique angles of sound incidence [6] and a method to find out the sound pressure reflection coefficient with a simultaneous measurement of sound pressure and particle velocity at nearly the same place [7]. This paper presents a measurement method to obtain acoustic properties at oblique angles of sound incidence by means of a separation of the incoming and reflecting impulse by a subtraction technique. The theory of the method is given and the measurement set-up for the determination of the acoustic properties at oblique sound incidence is presented. Results at perpendicular sound incidence are shown in comparison to the acoustic properties obtained with impedance tube following ISO 10534-2. Furthermore, measurement results of the sound absorption coefficient at oblique angle of sound incidence compared to an analytic solution will be discussed.

Theory

The schematic of the subtraction method is shown in Fig. 1. A loudspeaker is positioned at a certain distance h_y in front of a sample under consideration. Moreover, a microphone is placed at r_y above the sample. The angle between the loudspeaker and the microphone in respective to the normal surface of the surface is Θ. Because the acoustic properties of the surface are different to the ones of the surrounding medium, there will be reflection at the surface. This is taken into account by introducing an image source. The impulse response of the measurement system can be identified by either using a Maximum Length Sequence (MLS) and performing a cross-correlation of the measured pressure and the excitation signal or using a sine sweep and performing a deconvolution. The cross-correlation can be carried out by using the Hadamard transform. The loudspeaker is

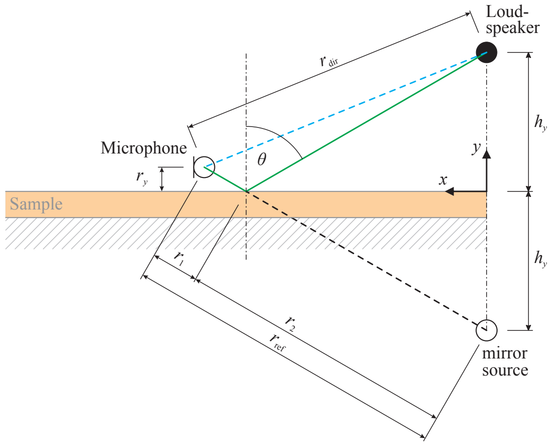

Figure 1: Schematic of the measurement system.

excited by an input signal $x_e(t)$ and the pressure at a distance of $r_{\rm dir}$ is recorded by means of a microphone. In a first step, a free field measurement (impulse response $h_{\rm ff}$) is performed. The measured pressure

$$p_{\rm ff}(t) = x_{\rm e}(t) * h_{\rm ff}(t) = p_{\rm ff,d}(t) + p_{\rm ff,p}(t) \qquad (1)$$

in a free field consists of a direct $p_{\rm ff,d}$ and a parasitic part $p_{\rm ff,p}$. Thereby, the symbol $*$ denotes the convolution. The parasitic part represents reflections at objects and the walls of the room. Furthermore, the measurement is repeated with a sample placed as shown in Fig. 1. The measured pressure above the sample (impulse response $h_{\rm m}$)

$$p_{\rm m}(t) = x_{\rm e}(t) * h_{\rm m}(t) = p_{\rm m,d}(t) + p_{\rm m,r}(t) + p_{\rm m,p}(t) \quad (2)$$

is a superpositon of the direct, parasitic and the reflected component $p_{\rm m,r}$. The impulse responses of both measurement systems compute to

$$\begin{aligned} h_{\rm m}(t) &= p_{\rm m}(t) * x_{\rm e}(-t) \\ &= (h_{\rm m,d} + h_{\rm m,r} + h_{\rm m,p}) * \delta(t) \\ &= C_{\rm m,d}s(t) * \delta(t-\tau_1) + C_{\rm m,r}s(t) * r(t) * \delta(t-\tau_2) \\ &\quad + C_{\rm m,p}s(t) * f_{\rm p}(t) * \delta(t-\tau_3) \qquad (3) \\ h_{\rm ff}(t) &= p_{\rm ff}(t) * x_{\rm e}(-t) \\ &= (h_{\rm ff,d} + h_{\rm ff,p}) * \delta(t) \\ &= C_{\rm ff,d}s(t) * \delta(t-\tau_1) + C_{\rm ff,p}s(t) * f_{\rm p}(t) * \delta(t-\tau_3), \qquad (4) \end{aligned}$$

where δ is the dirac delta function, f_{p} is the parasitic component of the impulse response, s is the impulse response of the measurement system and r the impulse response of the sample. The coefficients $C_{\mathrm{m,d}}, C_{\mathrm{m,r}}, C_{\mathrm{m,p}}, C_{\mathrm{ff,d}}$ and $C_{\mathrm{ff,p}}$ compensate the amplitude and $\tau_{1,2,3}$ the time shift of a traveling spherical wave. The impulse response of each measurement system is a superposition of the direct (d), reflected (r) and parasitic (p) part of the impulse response, which are excited at different times ($\tau_1 < \tau_2 < \tau_3$). The parasitic part can be canceled out using a time window after the following subtraction of both impulse responses. To separate the reflected impulse response $h_{\mathrm{m,r}}$, the impulse responses (3) and (4) are subtracted. With the assumption that the direct impulse responses in both measurements are equal ($h_{\mathrm{m,d}} = h_{\mathrm{ff,d}}$) and neglecting the parasitic parts, the subtraction results in

$$g(t) = h_{\mathrm{m}}(t) - h_{\mathrm{ff}}(t) = C_{\mathrm{m,r}} s(t) * r(t) * \delta(t - \tau_2)\,. \quad (5)$$

To quantify the effectiveness of the subtraction result, the reduction factor [9]

$$RF = 10 \log \left(\frac{\int_{\tau_1-\Delta t}^{\tau_1+\Delta t} h_{\mathrm{ff}}^2 \mathrm{d}t}{\int_{\tau_1-\Delta t}^{\tau_1+\Delta t} g^2 \mathrm{d}t} \right) \quad (6)$$

is used. In (6), the square of the impulse responses in case of the free field measurement and the subtraction result from Δt before and Δt after the time of the direct sound peak τ_1 are compared. In case of a perfect subtraction, the subtracted impulse response g is zero and $RF \to \infty$. In Fig. 2 a sketch of the subtraction is displayed including the time windows for canceling the parasitic components out of the impulse responses. Moreover, the influence of varying environmental conditions between the two measurements resulting in a time ($\Delta\tau$) and amplitude (ΔC) shift can be seen. In case of $\Delta\tau = 0$ and $\Delta C = 0$, the subtraction result in (5) only consists of the reflected green peak and the parasitic components. In frequency

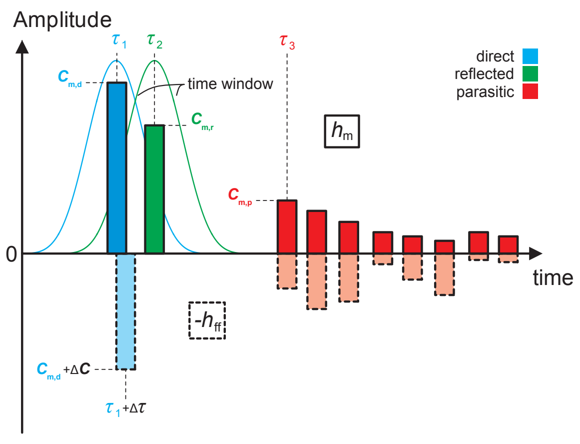

Figure 2: Sketch of the subtraction in (5) including the influence of varying environmental conditions between the two measurements and the time windows for canceling the parasitic components out of the impulse responses.

domain, (5) and the time windowed impulse response (4) compute to

$$H_{\mathrm{ff}}(\omega) = C_{\mathrm{ff,d}} S(\omega) e^{-j\omega\tau_1} \quad (7)$$
$$G(\omega) = C_{\mathrm{m,r}} S(\omega) R(\omega) e^{-j\omega\tau_2}\,. \quad (8)$$

Dividing (8) and (7), replacing the coefficients $C_{\mathrm{ff,d}} = 1/r_{\mathrm{dir}}$ and $C_{\mathrm{m,r}} = 1/r_{\mathrm{ref}}$ and the time delays $\tau_1 = r_{\mathrm{dir}}/c$ and $\tau_2 = r_{\mathrm{ref}}/c$ (c is the speed of sound of the surrounding medium), the sound pressure reflection coefficient computes to

$$R(\omega) = \frac{G(\omega)}{H_{\mathrm{ff}}(\omega)} \frac{r_{\mathrm{ref}}}{r_{\mathrm{dir}}} e^{jk(r_{\mathrm{ref}} - r_{\mathrm{dir}})}\,, \quad (9)$$

where k is the wave number of the surrounding medium. Thereby, the sound absorption coefficient

$$\alpha = 1 - |R|^2 \quad (10)$$

can be calculated by using (9).

Subtraction optimization

To improve the result, some corrections of the subtraction method are done. First, we do not use the assumption that the pressure amplitude of the loudspeaker decays by inverse distance and therefore we replaced $r_{\mathrm{ref}}/r_{\mathrm{dir}}$ in (9) by a measured amplitude decay. Second, an oversampling similar to the one proposed in [9] is used to find the most effective subtraction result using (6) and $\Delta t = 0.3$ ms. Instead of iterative increasing the oversampling factor, an oversampling with factor 10 is applied in all measurements to improve the subtraction result. In this oversampling optimization, a set of 10 impulse responses is available to apply (5), whereas the best result in respect to (6) is used. This time signal of the impulse response is furthermore being phase shifted in frequency domain and transformed back in time domain. Moreover, the amplitudes are adjusted before subtracting to get a better reduction factor and hence a better subtraction result. Variations in the environmental conditions result in a time shift ($\tau_1 \pm \Delta\tau$) and a modification in the amplitude ($C_{\mathrm{ff,d}} = C_{\mathrm{m,d}} \pm \Delta C$) of the direct component of the impulse responses, see Fig. 2. By using the described subtraction optimization, the influences of varying environmental conditions can be reduced.

Measurement set-up

The distance r_{dir} between loudspeaker and microphone is chosen to be 1 m and the microphone is placed at $r_y = 0.15$ m. Therefore, in case of perpendicular sound incidence, the direct and reflected peak in h_{m} will be at $\tau_1 \approx 2.92$ ms and $\tau_2 \approx 3.79$ ms. The distances are a trade-off between the time, the impulse response of the sample r can be evaluated before the first reflections are in g (the evaluation time is between τ_2 and τ_3) and the fact, that there is no overlapping of the direct and reflected part in this evaluated time slot. The measurements were performed in a stairwell at the TU Wien. The distance to the surrounding wall is 2 m, so the first parasitic parts in h_{m}

will be at $\tau_3 \approx 11.66$ ms. The sound pressure is recorded 20 s with 500,000 samples/s, where the excitation signal is a MLS. The used samples are rock wool plates with different thicknesses (40 mm, 50 mm, 60 mm and 100 mm). The total sample size is 4 m^2. A typical measurement set-up can be seen in Fig. 3. Measurements with the here presented set-up can only be used for a maximum angle of 70°, because of the limited crossbar length.

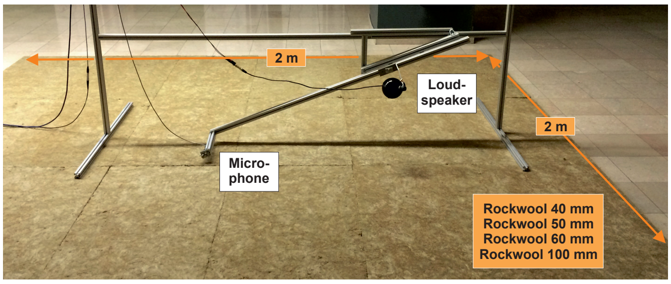

Figure 3: Typical measurement set-up in a stairwell at the TU Wien with a loudspeaker and microphone above a 4 m^2 rockwool sample.

Results and discussion

For canceling out the parasitic part of the impulse responses g and h_{ff}, a Blackman-Harris window with a length of 5 ms and a 3.5 ms Adrienne window is used. In Fig. 4 the sound absorption coefficient of a 40 mm rockwool sample with different time windows used for canceling of the parasitic part of the impulse response can be seen. The curve of the obtained sound absorption coefficient by using the Blackman-Harris window of course shows a different frequency resolution regarding the curve obtained by using the Adrienne window and looks more smooth. The Blackman-Harris window is a symmetric time window and its peak is placed at the point of the peak of the impulse response. The most important information of the sample's impulse response is located in the peak of the impulse response and there are more and more disturbances like reflections at the time after this peak. Hence, in the following, all calculations are done by using the Blackman-Harris window. The determined sound absorption coefficient can be measured up to 16 kHz but it can be seen that the value is getting 1 for higher frequencies. Thus, the sound absorption coefficient is only shown up to 10 kHz. The lower frequency limit (200 Hz) of the measurement results is bounded by the length of the time window.

Absorption coefficient at perpendicular sound incidence ($\Theta = 0°$)

The absorption coefficient at perpendicular sound incidence of rockwool samples with different thicknesses can be seen in Fig. 5. The result of the subtraction method is compared to the result of a measurement following ISO 10534-2 by using an impedance tube. It has to be mentioned that the impedance tube gives unreliable results for frequencies above 6.4 kHz, the frequency of the first transverse mode of the tube. Hence the impedance

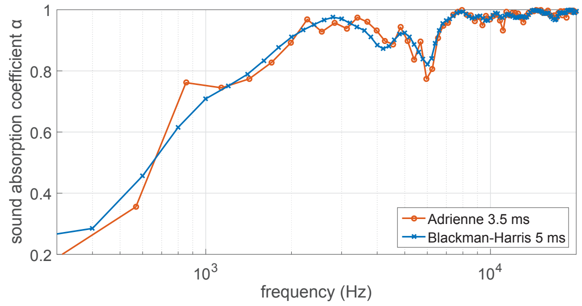

Figure 4: Sound absorption coefficient α of a 40 mm rockwool sample at perpendicular sound incidence $\Theta = 0°$ using a 5 ms Blackman-Harris window and a 3.5 ms Adrienne window.

tube results are just shown up to 6.4 kHz. The result of the subtraction method shows good agreement with the sound absorption coefficient obtained with the standardized measurement procedure. The curves obtained by the ISO of the samples with 50 mm and 60 mm seem to be shifted in frequencies regarding the one, obtained with the subtraction technique. To measure the sound absorption coefficient using ISO, a sample of 29 mm diameter has to be cutted out of the rockwool plate. Unfortunately, this can not be done very easy since the samples are limply and therefore, the cutting process cannot be performed very accurate. Nevertheless, the results of both methods match quite well.

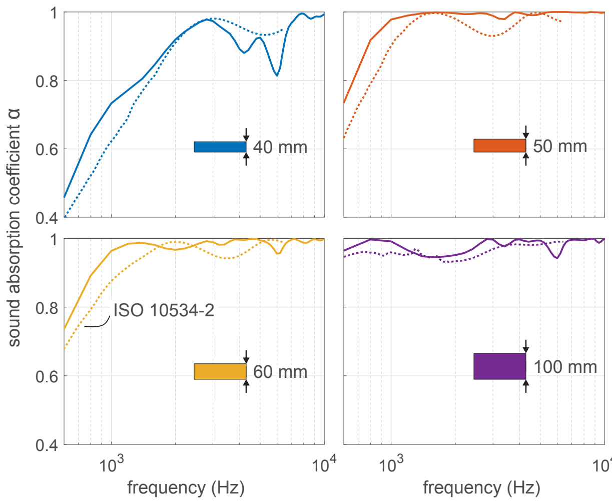

Figure 5: Measured sound absorption coefficient α of different rockwool plates at perpendicular sound incidence $\Theta = 0°$ using the subtraction method and ISO 10534-2 (dotted line).

Acoustic properties at oblique sound incidence

By means of the method following ISO 10534-2, only the acoustic properties at perpendicular sound incidence can be investigated. For a further validation of the subtraction method, the sound absorption coefficient at oblique sound incidence will be compared to the sound absorption coefficient using the Komatsu model of fibrous materials [10]. As an input for the Komatsu model, the flow resistivity of the samples given by the manufacturer with 8 kPa s/m^2 is used.

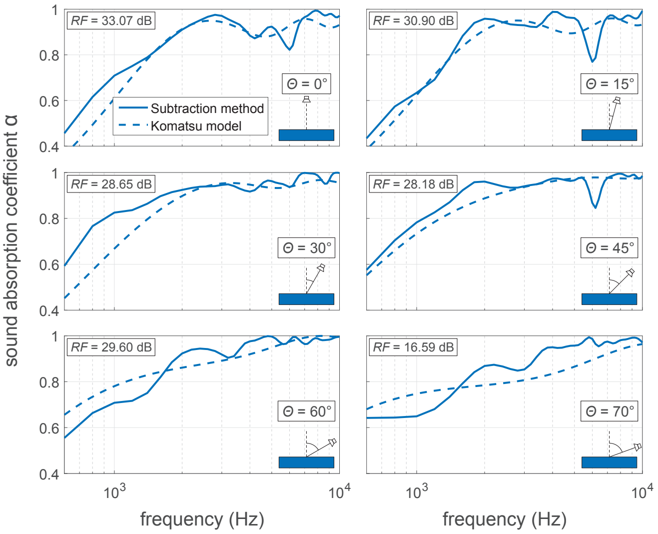

Figure 6: Measured sound absorption coefficient α of a 40 mm rockwool plate at oblique angles of sound incidence using the subtraction method and calculated using the Komatsu model (dashed line).

In Fig. 6, the measured sound absorption coefficient of the 40 mm rockwool sample at oblique angles of sound incidence in comparison to the calculated one using the Komatsu model can be seen. Moreover, the reduction factor of each measurement using (6) is shown. For measurements at the angle of sound incidence of 70°, the reduction factor decreases to about 17 dB, whereas the reduction factor at the remaining angles of sound incidence is at about 30 dB. According to [11], a reduction factor more than 10 dB is sufficient. The sound absorption coefficient increases with a rising angle of sound incidence up to an angle of 60° especially at low frequencies, because the wave has to cross more sound absorbing material at higher angles of sound incidence and thus more energy is absorbed. A drop in the sound absorption at 0°, 15° and 45° can be observed at about 6 kHz, probably caused by resonance effects in the plate. However, the measured values of the sound absorption coefficient match the theoretical values obtained by using the Komatsu model.

Conclusion

A fast and stable measurement method is presented to obtain acoustic properties at perpendicular as well as oblique sound incidence. In this method, only a sound source and one microphone is needed, which makes the method easy and cheap. No knowledge of the strength and directivity of the sound source is needed. Moreover, no special acoustic environment is needed, because the excitation with MLS is very robust. A full set of acoustic properties in a frequency range of 200 Hz to 16 kHz and sound incidence angles up to 70° can be achieved and used for a precise simulation of an acoustic field close to reality.

References

[1] ISO 354: Acoustics - Measurement of sound absorption in a reverberation room, 2003.

[2] ISO 10534-2: Acoustics - Determination of sound absorption coefficient and impedance in impedance tubes - Part 2: Transfer-function method, 1998.

[3] Metzger, J. and Kaltenbacher, M.: A comparison of measurement techniques to determine the acoustic impedance at oblique sound incidence angle. In: Proceedings of DAGA 2015 - 41st German Annual Conference on Acoustics, Nuremberg, Germany, 2015, p. 780-783.

[4] Tamura, M.: Spatial Fourier transform method of measuring reflection coefficients at oblique incidence. I: Theory and numerical examples, The Journal of the Acoustical Society of America 88, 1990, p. 2259-2264.

[5] Tamura, M., Allard, J. F. and Lafarge, D.: Spatial Fourier transform method for measuring reflection coefficients at oblique incidence. II. Experimental results, The Journal of the Acoustical Society of America 97, 1995, p. 2255-2262.

[6] Allard, J.F., Champoux, Y. and Nicolas, J.: Pressure variation above a layer of absorbing material and impedance measurement at oblique incidence and low frequencies, Journal of the Acoustical Society of America 86, 1989, p. 766-770.

[7] Lanoye, R., Vermeir, G. and Lauriks, W.: Measuring the free field acoustic impedance and absorption coefficient of sound absorbing materials with a combined particle velocity-pressure sensor, Journal of the Acoustical Society of America 119, 2006, p. 2826-2831.

[8] Mommertz, E.: Angle-dependent in-situ measurements of reflection coefficients using a subtraction technique, Applied Acoustics 46, 1995, p. 251-263.

[9] Robinson, P. and Xian, N.: On the subtraction method for in-situ reflection and diffusion coefficient measurements, The Journal of the Acoustical Society of America 129, 2010, p. 99-104.

[10] Komatsu, T.: Improvement of the Delany-Bazley and Miki models for fibrous sound-absorbing materials, Acoustical Science and Technology 29.2, 2008, p. 121-129.

[11] DIN EN 1793-5: Road Traffic Noise reducing devices - Test method for determining the acoustic performance - Part 5: Intrinsic characteristics - In situ values of sound reflection under direct sound field conditions, 2002.